NUREG/CR-4028
ANL-84-67

NUREG/CR-4028
ANL-84-67

UNIFIED THEORY FOR PREDICTING MAXIMUM FLUID PARTICLE SIZE FOR DROPS AND BUBBLES

by

G. Kocamustafaogullari, I. Y. Chen,
and M. Ishii

ARGONNE NATIONAL LABORATORY, ARGONNE, ILLINOIS
Operated by THE UNIVERSITY OF CHICAGO

Prepared for the Office of Nuclear Regulatory Research
U. S. NUCLEAR REGULATORY COMMISSION
under Interagency Agreement DOE 40-550-75

Argonne National Laboratory, with facilities in the states of Illinois and Idaho, is owned by the United States government, and operated by The University of Chicago under the provisions of a contract with the Department of Energy.

NUREG/CR-4028
ANL-84-67
(Distribution Codes: R2 & R4)

ARGONNE NATIONAL LABORATORY
9700 South Cass Avenue
Argonne, Illinois 60439

UNIFIED THEORY FOR PREDICTING MAXIMUM FLUID PARTICLE SIZE FOR DROPS AND BUBBLES

by

G. Kocamustafaogullari, I. Y. Chen,
and M. Ishii

Reactor Analysis and Safety Division

Report Completed: June 1984

Report Issued: October 1984

Prepared for the Division of Accident Evaluation
Office of Nuclear Regulatory Research
U. S. Nuclear Regulatory Commission
Washington, D. C. 20555
under Interagency Agreement DOE 40-550-75

NRC FIN No. A2026

UNIFIED THEORY FOR PREDICTING MAXIMUM FLUID PARTICLE SIZE FOR DROPS AND BUBBLES

by

G. Kocamustafaogullari, I. Y. Chen, and M. Ishii

ABSTRACT

A simple model is developed based on a two-dimensional linearized Kelvin-Helmholtz stability theory to describe the breakup of drops and bubbles in fluid media. Breakup is predicted to occur if the growth of disturbances at the interface is faster than the rate at which disturbances propagate around the interface to the side of particle. Agreement between the model and experimental data indicates that the principle physical mechanisms involved are properly accounted for by the model. The same theory is applicable to drops in liquid, drops in gas, and bubbles in liquid. The present analysis gives the first unified theory for fluid particle breakups which has not been available previously.

NRC FIN No. | Title

A2026 | Phenomenological Modeling of Two-phase Flow in Water Reactor Safety Research

TABLE OF CONTENTS

LIST OF FIGURES

LIST OF TABLES

NOMENCLATURE

NOMENCLATURE

Ar	Archimedes number
c	Complex wave celerity
c_i	Imaginary part of wave celerity
c_r	Speed of propagation
d	Diameter
d_e	Volume-equivalent sphere diameter
$(d_e)_{max}$	Maximum value of d_e at breakup
d_p	Twice the mean radius of curvature
Eo	Eötvös number
F	Dimensionless group defined by Eq. (58)
h	Fluid thickness
g	Gravitational acceleration
k	Wave number, $2\pi/\lambda$
k_m	Wave number at particle breakup
M	Morton number
N_μ	Viscosity number
P	Pressure
R_p	Mean radius of curvature
S	Maximum velocity gradient in the continuous fluid
t	Time
t_g	Growth time
t_p	Propagation time
u	Velocity
u_c	Rise or fall velocity
$u_{c\theta}$	Tangential component of u_c at the interface
We	Weber number

x	Horizontal coordinate axis
y	Vertical coordinate axis
ε	Energy dissipation per unit mass per unit time
$\lvert\Delta\rho\rvert$	Absolute value of density difference, $\lvert\rho_c - \rho_d\rvert$
η	Local wave amplitude
η_b	Wave amplitude at breakup
η'	Amplitude of initial disturbances
θ	Angular position
θ_o	Angular position of initial disturbances
θ_w	Wake angle
λ	Wave length
ρ	Mass density
σ	Surface tension
ϕ	Velocity potential

Subscripts

1	Lower fluid in Kelvin-Helmholtz instability
2	Upper fluid in Kelvin-Helmholtz instability
c	Continuous fluid
c_r	Critical value
d	Dispersed fluid
max	Maximum value
tr	Turbulent

Superscripts

'	Disturbances
*	Dimensionless variables

EXECUTIVE SUMMARY

Disturbances which cause fluid particle splitting are classified as rapid accelerations, high shear stresses and turbulent fluctuations in the continuous fluids. However, it has been observed that even when none of such external disturbances is present, there is a limit to the size to which drops and bubbles can reach. The maximum size attained by single bubbles or drops rising or falling freely through a stagnant media in the absence of such disturbances has been traditionally attributed to the instability of Rayleigh-Taylor instability, which does not take into account the effects of relative motion.

Based on the Kelvin-Helmholtz instability theory which allows a relative motion at the interface, a simple model is developed to describe the breakup of drops and bubbles falling or rising through a fluid. Breakup is predicted to occur if the growth of disturbances on the leading front is rapid enough relative to the propagation rate of disturbances around the interface. Based on this theoretical model and available experimental data, a simple correlation is developed to predict the maximum stable particle size in a fluid.

Predicted values of the maximum particle size are compared with experimental data for cases of bubbles in liquid, drops in liquid, and drops in gas. Agreement between the model and experimental results is favorable.

I. INTRODUCTION

Breakup and limiting size of fluid particles in dispersed two-phase flow systems including the liquid-liquid particulate systems are important factors in determining the fluid particle size distribution and hence the effectiveness of the interfacial mass, momentum, and energy transports. A knowledge of the disintegration of drops and bubbles is essential to the eventual understanding of the interfacial transfer mechanisms and two-phase flow pattern transitions in many important engineering systems of interest to various branches of technology and science. Engineering applications include gas-liquid droplet systems, such as atomizers, dryers, absorbers, wet steam separators and cryogenic heat exchangers, liquid-liquid droplet systems, such as liquid-liquid extractors, separators used with distillation columns, and packed towers when the packing is not wetted by the disperse phase, and finally liquid-gas (or vapor) bubbly systems, such as boiling water and pressurized water nuclear reactors, boilers, evaporators, flash distillation and aeration units. Although drops and bubbles seldom occur in isolation in such systems, it is essential to understand the behavior of a single fluid particle before a full knowledge of interacting drops and bubbles can be achieved.

As discussed in the next section in greater detail, disturbances which cause fluid particle splitting are classified as rapid accelerations, high shear stresses and turbulent fluctuations in the surrounding continuous fluids. However, it has been observed that even when none of such obvious disturbances is present, there is a limit to the size to which drops and bubbles can reach. The maximum size attained by a single bubble or a drop rising or falling freely through stagnant media in the absence of such disturbances has been attributed to the instability of standing waves developed at the particulate-continuous fluids interface, i.e., Rayleigh-Taylor instability.

It is to be noted here that Rayleigh-Taylor instability applies to a case with no relative motion between two superposed fluid layers. However, in reality, even for the breakup in stagnant media there exists a relative motion between particulate and continuous fluids, and disturbances which grow by time are generated due to a relative motion. Kelvin-Helmholtz instability theory allows a relative motion between two superposed fluid layers. Disturbances generated by this instability propagate at the interface with a certain speed.

Extending this Kelvin-Helmholtz instability theory, it is the objective of this study to develop a simple model to predict the maximum fluid particle size rising or falling in fluid media. The correlation thus developed is general in the sense it can be used for liquid-gas, liquid-liquid, and gas-liquid system.

II. FLUID PARTICLE BREAKUP MECHANISMS

To determine the limiting size of fluid particles a number of processes which may cause breakup of fluid particles have been identified. The most important mechansims are classified as follows:

A. Breakup in Gas Flow Fields,
B. Breakup in Viscous Flow Fields,
C. Breakup in Turbulent Flow Fields,
D. Breakup in Stagnant Fluids.

A. Breakup in Gas Flow Fields

This mechanism of breakup applies to drops suddenly exposed to a high velocity gas stream (including shock waves). The investigation of the bursting of drops in an air stream has a long history, dating back to before 1904. Large free-falling drops in still air, or somewhat smaller drop in a steady stream of air, were first considered by Lenard [1] and by Hochshwender [2]. Since then this breakup process has been studied both experimentally and theoretically [3-9]. According to this breakup mechanism, gas flowing over the surface of a liquid droplet causes the dynamic pressure normal to the surface of the droplet to be nonuniform, resulting in a deformation of the liquid drop. If the pressure forces cause a distortion severe enough to overcome the surface tension and viscous forces within the liquid, the liquid drop will eventually split. Hence it was concluded that breakup is controlled by the dynamic pressure, surface tension and viscous forces. For liquids with slight viscosity effects, the deformation and breakup of drops are predominantly determined by a single dimensionless group, the Weber number. Results of various experimental investigations can be expressed by a simple Weber number criterion, indicating that drops will break when

$$We_{cr} = \text{constant} \qquad (1)$$

with the critical Weber number defined by

$$We_{cr} \equiv \frac{\rho_c (d_e)_{max} (u_c - u_d)^2}{\sigma} \tag{2}$$

where $(u_c - u_d)$ is the relative velocity between the continuous and the particulate phase, $(d_e)_{max}$ is the limiting volume-equivalent drop diameter, σ is the surface tension, and ρ_c is the mass density of the continuous phase.

From the data of Merrington and Richardson [3], Hinze [4] has estimated the constant appearing in Eq. (1) to be 13 for low-viscosity liquids. This may be compared with the value of 10.6 from the data of Lane [6], 10.3 for mercury drops in air, obtained by Haas [8], and 7.2 to 16.8 (with an average of about 13.0) for water, methyl alcohol, and a low-viscosity silicone oil obtained by Hanson et al. [5].

Hinze [7] considered the effect of viscosity and suggested that the critical Weber number should be a function of a dispersed phase viscosity group. For this relation the following form is chosen

$$We_{cr} = We_{cr}\big|_{\mu=0} \left[1 + f(N_{\mu d})\right] \tag{3}$$

where $N_{\mu d}$ is the viscosity number based on dispersed phase. It is defined as

$$N_{\mu d} \equiv \frac{\mu_d}{\rho_d \, d_{max} \, \sigma} \tag{4}$$

where μ_d and ρ_d, respectively, are the dynamic viscosity and mass density of the dispersed phase. $We_{cr}\big|_{\mu=0}$ is the value of the critical Weber number for vanishing viscosity effect of the drop, which is equal to the constant appearing in Eq. (1). The data of Hanson et al. [5] give only a qualitative support to the effect, but do not agree in detail. A slightly different empirical relation [10] given by the following expression has also been proposed

$$We_{cr} = We_{cr}\Big|_{\mu=0} + 14\, N_{\mu d} \tag{5}$$

which is good to a maximum deviation of approximately 20% at the higher viscosity end.

B. Breakup in Viscous Flow Fields

This mechanism of breakup applies to fluid particles surrounded by viscous fluid where there exists strong velocity gradient in the vicinity of the particle. In this case the continuous fluid Reynolds number is so small that the dynamic forces are no longer important, and the breakup is controlled by the viscous shear and surface tension forces. If the viscous shear force is large enough, the interfacial tension forces are no longer able to maintain the fluid particle intact, and it ruptures into two or more smaller particles.

The first fundamental work on the splitting of drops and bubbles under the action of surface tension and viscous forces were made by Taylor [11] in 1934. His test apparatus was designed to generate carefully controlled flow patterns. One of these consisted of Couette flow and the other was a plane hyperbolic flow. A variety of liquids with different viscosities were used. Taylor made numerous observations, many of which subsequently explained by Tomotika [12]. The results can be summarized as follows:

a. Under the action of viscous shear, a drop alongates into the shape of a prolate ellipsoid of revolution.

b. The deformation is determined by the Weber number based on the velocity gradient defined as

$$We_{\nu} = \frac{\mu_c S d}{\sigma} \tag{6}$$

where μ_c is the absolute viscosity of the continuous phase, and S is the maximum velocity gradient in the continuous fluid flow field.

c. The breakup of the fluid particles occurs at a critical value of the Weber number which depends on the continuous fluid flow field, and Taylor has studied the deformation of a single drop as a function of S; he determined the value of S at which the breakup of the drop occurs.

Although the basic principle of the breakup mechanism is correctly predicted, Taylor's theory has been modified over the years [13-15]. For example, Rumscheidt and Mason [13] proposed that breakup occurs if We_v exceeds a critical value given by

$$We_v = \frac{1 + (\mu_d/\mu_c)}{1 + (19/16)(\mu_d/\mu_c)} \tag{7}$$

which varies only between 1.0 and 0.82 as (μ_d/μ_c) varies from zero to infinity.

It should be noted here that the Taylor mechanism of fluid particle deformation applies if both the undeformed and elongated drops are small compared with local regions of viscous flow. When the Reynolds number of the external flow field is large, as it is in most practical applications, the spatial dimensions of such local regions are very small compared with the drop sizes. Under these circumstances, the determining factor is the dynamic pressure caused by the velocity changes over distances of the order of the fluid particle diameter.

C. Breakup in Turbulent Flow Fields

According to the disintegration mechanism of fluid particles in an external turbulent flow field it is assumed that the dynamic pressure forces of the turbulent motions are the factor determining the size of the largest fluid particle. These dynamic pressure forces are caused by changes in velocity over distances within the diameter of a particle. Kolmogorov [17], and Hinze [7] took this view, and further assumed that since the break up was to be considered local, the principles of local isotropic turbulence would be valid. Under these circumstances, Hinze defined a Weber number based on the local turbulent fluctuations as

$$We_{tr} \equiv \frac{\rho_c \overline{(\Delta u)^2}\, d_e}{\sigma} \tag{8}$$

where $\overline{(\Delta u)^2}$ is the spatial average value of the square of velocity differences over a distance equal to particle diameter. To relate this average kinetic energy to this distance, Hinze used Kolmogorov's universal equilibrium theory to show that

$$\overline{(\Delta u)^2} = 2.0\ (\varepsilon d_e)^{2/3} \tag{9}$$

where ε is the energy dissipation per unit mass and time. Assuming that a constant critical Weber number criterion still applies, from Eqs. (8) and (9) Hinze obtained

$$(d_e)_{max} \left(\frac{\rho_c}{\sigma}\right)^{3/5} \varepsilon^{2/5} = C \tag{10}$$

He used experimental results due to Clay [17] to calculate the value of the constant C. Clay's apparatus consisted of two coaxial cylinders, one of which, namely, the inner one rotated. The space between the cylinders was filled with two immiscible fluids, one of which formed discrete drops. Clay found the maximum drop size as a function of energy input into the liquid. On the basis of these data Hinze found that C = 0.725, and, hence the critical Weber number can be given by

$$(We_{tr})_{cr} \equiv \frac{\rho_c\ \overline{(\Delta u)^2}\ (d_e)_{max}}{\sigma} = 2\ \rho_c\ \varepsilon^{2/3}\ (d_e)_{max}^{5/3} = 1.18 \tag{11}$$

It must be noted that data on breakup in an isotropic turbulent field are nonexistent, so direct verification of the criterion is not possible. Sleicher [18] has shown that Eq. (11) is not valid for pipe flow. The breakup occurs in the vicinity of a wall, where the conditions are the farthest from the approximate isotropic conditions at the center line. The breakup for a pipe system is probably a result of a balance among surface forces, velocity fluctuations, dynamic pressure fluctuations, and the steep velocity gradients,

i.e., a result of a combination of the various breakup mechanisms summarized above.

The work of Kolmogorov and Hinze concerned with the splitting of drops and bubbles by turbulent flow has been modified by Sevik and Park [19]. They suggested that resonance can cause bubble and drop break in turbulent flow fields when the characteristic turbulence frequency matches the lowest or natural frequency mode of an entrained fluid particle. Since damping is very small, such drops or bubbles will deform very violently if the existing frequency corresponds to one of their resonant frequencies. By setting a characteristic frequency of the turbulence equal to such a resonant frequency, they predict theoretically the critical Weber numbers corresponding both Clay's droplet splitting experiments and their bubble splitting experiments. It was found for droplets

$$(We_{tr})_{cr} = 1.04 \tag{12}$$

and for bubbles

$$(We_{tr})_{cr} = 2.6 \tag{13}$$

It should be noted that Hinze calculated a value of 1.18 based on tests involving the dispersion of various immiscible liquids, and that the critical Weber number for bubble breakup in turbulent flow fields is greater than that for drop breakup by about a ratio of 2.5.

D. Breakup in Stagnant Fluids

In the foregoing breakup mechanisms, disturbances which cause particle splitting are due to rapid acceleration, high shear stresses, and turbulent fluctuations in the continuous surrounding fluids. It has been observed that even when none of such external disturbances are present, there is a limit to the size to which drops and bubbles can reach. The maximum size attained by a single bubble and drop rising or falling freely through stagnant media in the absence of such disturbances has been attributed to Rayleigh-Taylor instability [20-30].

Rayleigh-Taylor instability can occur when a heavier fluid overlies on a lighter one. Hence it is always the advancing interface of a freely moving

bubble or drop (whether rising or falling under gravity) that is prone to the interfacial instability by this mechanism. The instability manifests itself as an indentation at the leading front surface (the upper surface for rising bubbles or drops and the lower surface for falling drops) which grows deeper as time advances, and eventually leads to a breakup of fluid particles.

This type of breakup mechanism was first considered by Komabayashi et al. [20] to determine the maximum size of falling drops in air. It was found that the maximum diameter was 0.855 cm for falling water drops in air. This theoretical finding was in good agreement with the experimental observations of Pruppacher and Pitter [21]. This theory has been extended over the years by others [22-30]. For example, the following simple equation for the maximum diameter of falling drops was suggested by Grace et al. [29],

$$(d_e)_{max} = 4\left(\frac{\sigma}{g\Delta\rho}\right)^{1/2} \tag{14}$$

where $(d_e)_{max}$ is the volume equivalent diameter at the breakup.

Equation (14) yields relatively good agreement with the experimental data on falling drops in air and in low viscosity liquids [3,29,31-35]. However, it was observed that the predictions made by Eq. (14) were in grave error for rising bubbles or drops [29]. In some of the analyses the Rayleigh-Taylor instability theory has been introduced with a tangential motion of the disturbance along the interface [29,30]. It was postulated that the breakup is to occur if the growth of indentations on the leading edge is rapid enough relative to the rate at which the disturbance is carried around the interface to the equator of a fluid particle. A semi-empirical relation was developed to predict the maximum particle diameter in which a constant was correlated using existing experimental data. It was found that the data for bubbles requires a different constant, 3.8, than the data for liquid drops. For the latter case, the optimum value of the constant was found to be 1.40.

It is important to note that in this type of analyses the breakup criteria were based on the growth of the standing waves, i.e., Rayleigh-Taylor instability, where there is no relative velocity permitted between the particulate and continuous phases. However, in reality, even during the breakup in stagnant media there exists a relative motion between two phases, and the

disturbances are generated at the interface due to a relative motion between two phases. Therefore, the use of the Rayleigh-Taylor instability analysis seems inconsistent in this case. It is natural to expect an effect of the relative velocity on the wave propagation and breakup process. By taking this view, a new breakup mechanism is proposed here in terms of progressive waves, namely, Kelvin-Helmholtz instability, which allows a relative motion between two superposed fluid layers.

In what follows we shall develop a Kelvin-Helmholtz instability analysis applicable to fluid particle deformations and utilize it to determine the maximum size of fluid particles rising or falling in a fluid.

III. KELVIN-HELMHOLTZ INSTABILITY

The stability of two superposed inviscid fluids flowing with different velocities will be considered here. It was Helmholtz (1868) who first considered the stability of the vortex sheet at the interface of the two superposed semi-inifinite fluids flowing with different velocities. His work was followed by that of Kelvin (1871), and this type of instability is known as Kelvin-Helmholtz instability. Derivations presented here will closely follow Yih [36], where the stability of the two-superposed fluids with semi-infinite depth was studied. Hence, only the essential features of the development are given here.

The stability of two superposed incompressible, inviscid fluids to be considered here is illustrated in Fig. 1. The lower fluid is identified by subscript 1 and the upper fluid by 2. The fluids are flowing concurrently in a horizontal, constant area channel. The velocities of the two fluids are assumed to be horizontal in direction, and are denoted by u_1 and u_2, respectively. If the effects of viscosity of the fluids are neglected, and the perturbed flow is assumed to be irrotational, the velocity potentials, ϕ, of each fluid satisfy the two dimensional Laplace equation. Thus,

$$\frac{\partial^2 \phi_i}{\partial x^2} + \frac{\partial^2 \phi_i}{\partial y^2} = 0 \ , \ i = 1, 2 \tag{15}$$

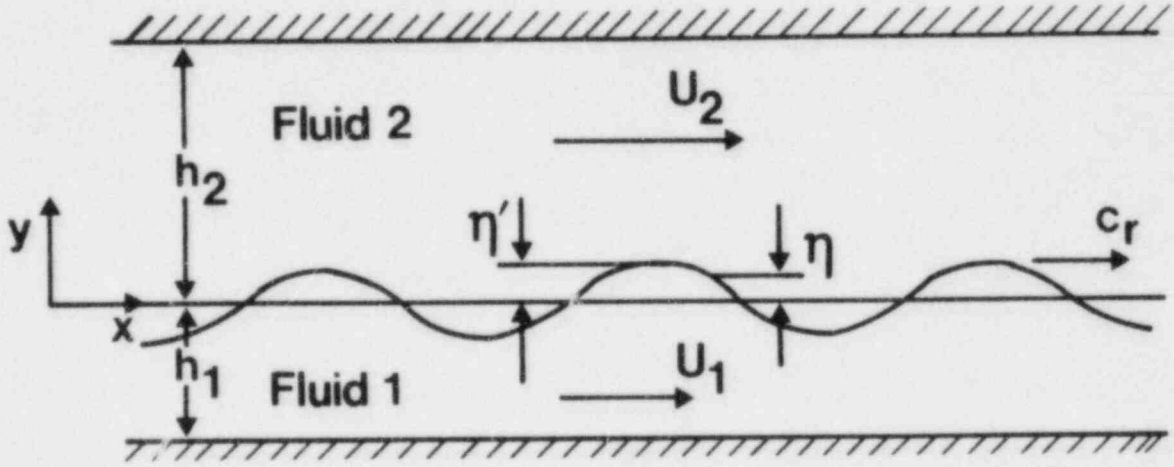

Fig. 1. Stability of Two Superposed Fluids Flowing with Two Different Velocities

in which x is measured in the mean flow direction, and y measures the vertical distance from the undisturbed interface. Denoting the perturbed quantities about the steady state solution by a prime symbol, the velocity potentials can be written as

$$\phi_i = u_i\, x + \phi_i' \,, \quad i = 1, 2 \tag{16}$$

If η is the displacement of the interface in the vertical y direction, the kinematic interfacial condition to be satisfied at $y = 0$ is

$$\frac{\partial \eta}{\partial t} + u_i \frac{\partial \eta}{\partial x} = \frac{\partial \phi_i}{\partial y} \,, \quad i = 1, 2 \tag{17}$$

in which quadratic terms in η and ϕ_i's are neglected. Other boundary conditions for ϕ_1' and ϕ_2' are

$$\text{at } y = -h_1 \qquad \frac{\partial \phi_1'}{\partial y} = 0 \tag{18}$$

$$\text{at } y = h_2 \qquad \frac{\partial \phi_2'}{\partial y} = 0 \tag{19}$$

which guarantee the vanishing normal velocity components at solid surfaces.

The dynamic boundary condition at the interface is given by

$$P_1 - P_2 = -\sigma \frac{\partial^2 \eta}{\partial x^2} \tag{20}$$

where terms of higher order than the first in η are neglected. Since the flow is assumed to be irrotational, the Bernoulli equation can be used to evaluate the pressures. The linearized form of it can be expressed for each fluid as follows:

$$\frac{P_i}{\rho_i} = -\frac{\partial \phi_i'}{\partial t} - u_i \frac{\partial \phi_i'}{\partial x} - gy \tag{21}$$

Evaluating Eq. (21) at the interface, $y = \eta$, for each fluid, and using the resulting equations in Eq. (19), one has

$$\rho_1 \left(\frac{\partial \phi_1'}{\partial t} + u_1 \frac{\partial \phi_1'}{\partial x} + g\eta \right) - \rho_2 \left(\frac{\partial \phi_2'}{\partial t} + u_2 \frac{\partial \phi_2'}{\partial x} + g\eta \right) = \sigma \frac{\partial^2 \eta}{\partial x^2} \tag{22}$$

This completes the formulation of the problem. If the perturbation is assumed to be periodic in x, the appropriate forms ϕ_1', ϕ_2' and η are

$$\phi_1' = a_1 \cosh[k(y + h_1)] \exp[ik(x - ct)] \tag{23}$$

$$\phi_2' = a_2 \cosh[k(y - h_2)] \exp[ik(x - ct)] \tag{24}$$

and

$$\eta = \eta' \exp[ik(x - ct)] \tag{25}$$

where k is the wave number which is related to the wave length, λ, by $k = 2\pi/\lambda$, and η' is the perturbation amplitude of the interface. Furthermore, a_1 and a_2 are integration constants to be determined by the boundary conditions, and c is the complex wave celerity defined as

$$c = c_r + i\, c_i \tag{26}$$

where c_r denotes the velocity of propagation of the wave in the x-direction whereas kc_i is the growth factor which determines the degree of amplification or damping. The disturbances are damped if $kc_i < 0$ and the mean flow is stable, the disturbances are amplified if $kc_i > 0$ and the mean flow is unstable. Finally, the mean flow is said to be neutrally stable, in which the disturbances are neither damped nor amplified, if $kc_i = 0$.

It is evident that ϕ_1' and ϕ_2' satisfy the Laplace equation, Eq. (15), and that the boundary conditions expressed by Eqs. (18) and (19) at $y = -h_1$ and $y = h_2$ are satisfied. In view of Eqs. (18)-(20) and (17), the integration constants a_1 and a_2 are determined. Hence,

$$a_1 = \frac{i\,(u_1 - c)\,\eta'}{\sinh(kh_1)} \tag{27}$$

and

$$a_2 = -\frac{i\,(u_2 - c)\,\eta'}{\sinh(kh_2)} \tag{28}$$

In view of Eqs. (27) and (28), the velocity potentials become

$$\phi_1' = \frac{i\,(u_1' - c)}{\sinh(kh_1)} \cosh[k(y + h_1)]\,\eta \tag{29}$$

and

$$\phi_2' = -\frac{i\,(u_2' - c)}{\sinh(kh_2)} \cosh[k(y - h_2)]\,\eta \tag{30}$$

It is to be noted that the potentials given by Eqs. (29) and (30) have been obtained through the kinematics of the respective flow fields. The dynamic interfacial condition, Eq. (22), has not been introduced yet. Hence one cannot say anything about the stability of the flow configuration.

Introducing Eqs. (29), (30) and (25) in Eq. (22), and solving the resulting equation for c, one obtains

$$c = \frac{\rho_1 \coth(kh_1)\, u_1 + \rho_2 \coth(kh_2)\, u_2}{\rho_1 \coth(kh_1) + \rho_2 \coth(kh_2)} \pm \left\{ \frac{\sigma k^2 + g(\rho_1 - \rho_2)}{[\rho_1 \coth(kh_1) + \rho_2 \coth(kh_2)]k} \right.$$

$$\left. - \frac{\rho_1 \rho_2 \coth(kh_1) \coth(kh_2) (u_1 - u_2)^2}{[\rho_1 \coth(kh_1) + \rho_2 \coth(kh_2)]^2} \right\}^{1/2} \qquad (31)$$

For the case of two superposed semi-infinite fluids, i.e., $h_1 \to -\infty$ and $h_2 \to \infty$, Eq. (31) reduces to that given in Yih [36] and Lamb [37]. In the absence of currents, Eq. (31) reduces to the Rayleigh-Taylor stability criterion when $\rho_1 < \rho_2$.

In view of Eqs. (26) and (31), c_r and c_i can be determined. Hence,

$$c_r = \frac{\rho_1 \coth(kh_1)\, u_1 + \rho_2 \coth(kh_2)\, u_2}{\rho_1 \coth(kh_1) + \rho_2 \coth(kh_2)} \qquad (32)$$

and

$$c_i = \left\{ \frac{\rho_1 \rho_2 \coth(kh_1) \coth(kh_2) (u_1 - u_2)^2}{[\rho_1 \coth(kh_1) + \rho_2 \coth(kh_2)]^2} - \frac{\sigma k^2 + g(\rho_1 - \rho_2)}{k[\rho_1 \coth(kh_1) + \rho_2 \coth(kh_2)]} \right\}^{1/2} \qquad (33)$$

Stability of the flow configuration can be analyzed by the behavior of c_i.

IV. PARTICLE BREAKUP CRITERION

A. Modeling

Even for the case of freely rising bubbles and drops, and falling drops in a stagnant media there exists a relative motion between fluid particles and

its surrounding fluid. Hence, any interfacial stability analysis used for a breakup mechanism should take into account the effect of the relative motion. Taking this view a breakup mechanism based on Kelvin-Helmholtz instability of interfacial progressive waves rather than the instability of standing waves will be developed here.

For the analysis, a series of approximations will be introduced as follows:

a. The compressibility of dispersed and continuous fluids is neglected.

b. The effects of viscosity in both dispersed and continuous fluids are neglected. Hence, the breakup criterion will not be expected to hold for extremely high viscous fluids.

c. The circulation within the fluid particle is neglected.

d. The effects of fluid particle advancing front curvature are neglected except insofar as it determines the value of tangential velocity component. It can be argued that these effects are of minor consequence for drops and bubbles which are sufficiently large for breakup to be a factor.

e. As discussed in greater detail in Section II, the breakup of fluid particles in a stagnant fluid proceeds from the advancing interfacial surface, i.e., from the upper surface for rising bubbles and drops and from the lower surface for falling drops, which is in agreement with most observations. Hence, it is assumed here that it will always be the advancing interface of a freely moving particle that is prone to instability.

Under these conditions the plane flow Kelvin-Helmholtz instability developed in the preceeding section can be applied. Identifying the continuous and dispersed fluids by subscripts c and d, respectively, the results obtained for the speed of propagation, c_r, and the growth factor, kc_i, can be expressed as follows:

$$c_r = \frac{\rho_c \coth(kh_c)\, u_c + \rho_d \coth(kh_d)\, u_d}{\rho_c \coth(kh_c) + \rho_d \coth(kh_d)} \tag{34}$$

$$kc_i = \left\{ \frac{\rho_c\, \rho_d \coth(kh_c) \coth(kh_d)\, k^2\, (u_{c\theta} - u_{d\theta})^2}{[\rho_c \coth(kh_c) + \rho_d \coth(kh_d)]^2} \right.$$

$$- \frac{\sigma k^3 - g|\Delta\rho|k}{\rho_c \coth(kh_c) + \rho_d \coth(kh_d)} \Bigg\}^{1/2} \tag{35}$$

where $(u_{c\theta} - u_{d\theta})$ is interpreted as the tangential velocity difference at the interface.

Now consider a cap bubble rising in stagnant liquid as illustrated in Fig. 2. Here a cap bubble is chosen for the purpose of reference. The present theory will be equally applicable to rising or falling drops with spherical or ellipsoidal shapes. In Fig. 2, θ_ω represents the wake angle of a cap bubble and R_p denotes the particle radius.

Using the potential flow theory for flow around a spherical particle, it can be shown that the tangential velocity components at an angular position of θ can be given by

$$u_{c\theta} = \frac{3}{2} u_c \sin\theta \tag{36}$$

$$u_{d\theta} = 0 \tag{37}$$

where it has been assumed that the circulation within the fluid particle is negligible.

It is noted here that the surrounding fluid dimension is much larger than the particle size. Thus

$$h_c \to \infty \tag{38}$$

Furthermore, for large arguments $\coth(kh_c)$ can be approximated by

$$\coth(kh_c) = 1.0 \tag{39}$$

In view of Eqs. (36) through (39), Eqs. (34) and (35) can be approximated by

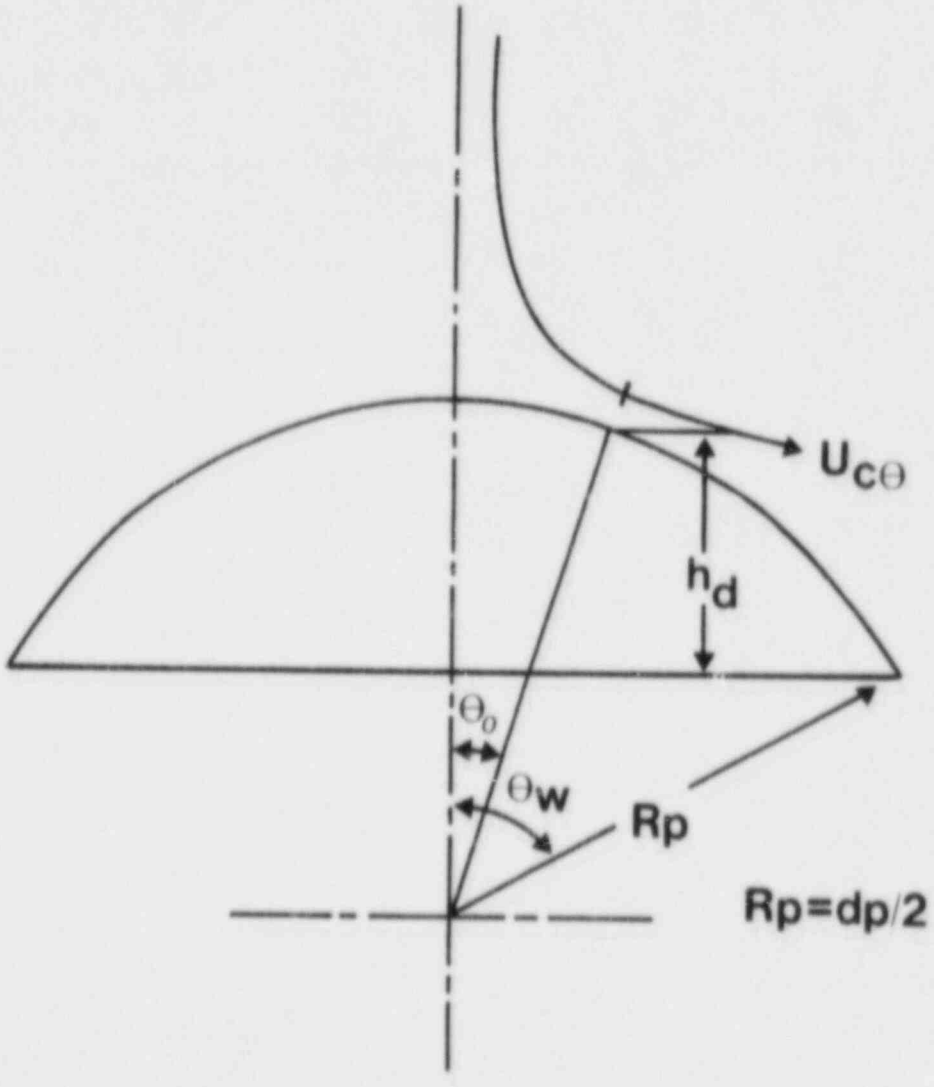

Fig. 2. Flow Around a Rising Cap Bubble

$$c_r = \frac{3}{2} \frac{\rho_c u_c \sin\theta}{\rho_c + \rho_d \coth(kh_d)} \tag{40}$$

$$kc_i = \left\{ \frac{\rho_c \rho_d \coth(kh_d) k^2 (\frac{3}{2} u_c \sin\theta)^2}{[\rho_c + \rho_d \coth(kh_d)]^2} - \frac{\sigma k^3 - g|\Delta\rho|k}{\rho_c + \rho_d \coth(kh_d)} \right\}^{1/2} \tag{41}$$

It is evident from Eqs. (40) and (41) that the speed of propagation as well as the growth factor depend upon the local angular position, original disturbance location, and the dispersed phase fluid thickness at the origination of disturbances. Referring to Fig. 2, it can be shown that h_d is given by the following equation.

$$h_d = \frac{d_p}{2} [\cos\theta - \cos\theta_\omega] \tag{42}$$

Here d_p is given in terms of the mean radius of curvature as $d_p = 2R_p$.

Equation (41) represents the growth factor of Kelvin-Helmholtz instability as applied to a rising cap bubble. Thus when $(kc_i) > 0$, the flow configuration is unstable. It should be emphasized here that the above stability criteria represents only the first step in developing a correlation for the breakup of a fluid particle interface. This information simply indicates when these interfacial waves occur and what their growth rates are. However, the appearance of the wave on the interface does not necessarily imply that it leads to drastic changes at the interface such as the breakup of particles. To answer this question of whether the waves can lead to a breakup or not, it is necessary to know the time required for these waves to grow to a certain amplitude so that splitting eventually can occur.

B. Breakup Criterion

A mathematical model is proposed here to predict the point at which breakup will be attained under given conditions. If t_g denotes the time at which the instability at the interface lead to a breakup t_g can be calculated from the wave form given by Eq. (25). Thus,

$$t_g = \frac{1}{kc_i} \ln(\eta_b/\eta') \tag{43}$$

where η_b is the amplitude at which breakup occurs. In a linearized stability analysis as it is the case here, there is no way to predict the value of (η_b/η') purely on theoretical basis. This implies that some experimental information on the initial disturbance amplitude is necessary to determine this quantity.

Disturbances originate near the top of the roof of a bubble and propagate down to the periphery with the local speed of propagation, c_r. In practice a bubble does not split unless the disturbance has grown sufficiently before the tip of the growing spike reaches the side of the bubble. If the wave travels to the end of a cap bubble or to the equator of a spherical particle without causing a breakup, it will be swept away at the edge into the continuous fluid. An estimate of the likelihood of splitting may be obtained by comparing the time required for a disturbance to grow with the time available for the growth. If t_p represents the time available for growth, that is the time required for a disturbance to travel from its origination to the side of the bubble, t_p can be calculated by

$$t_p = \int_{\theta_o}^{\theta_\omega} \frac{d_p}{2\, c_r}\, d\theta \tag{44}$$

where θ_o is the angular position where disturbances initiate. In view of Eq. (40) it can be shown that t_p can be calculated by

$$t_p = \left\{\frac{\rho_c + \rho_d \coth(kh_d)}{\rho_c\, u_c}\right\} d_p \ln\left\{\frac{\tan(\theta_\omega/2)}{\tan(\theta_o/2)}\right\} \tag{45}$$

The likelihood of a breakup may now be assessed by comparing the values of t_g and t_p. Thus a bubble tends to breakup by a disturbance for which

$$t_p > t_g \tag{46}$$

Combining Eqs. (43) and (45) with Eq. (46), a breakup criterion may be expressed as

$$(kc_i)\left\{\frac{\rho_c + \rho_d \coth(kh_d)}{\rho_c u_c}\right\} d_p \ln\left\{\frac{\tan(\theta_\omega/2)}{\tan(\theta_o/2)}\right\} > \ln(\eta_b/\eta') \tag{47}$$

Assuming that the terminal velocity, u_c, initial disturbance position, θ_o, and amplitude ratio, (η_b/η'), are expressible in terms of the particle diameter, basically there are two variables in Eq. (47), namely, the wave number and the particle diameter. It is usual practice in linearized stability analysis to consider the wave number which causes the most unstable wave growth. That is the value of k calculated by

$$\frac{d(kc_i)}{dk} = 0 \tag{48}$$

However, when Eq. (48) is solved for a given diameter it has been observed that the most unstable wave number is so small that the corresponding wave length, $\lambda = 2\pi/k$, becomes longer than a half of the circumference. This implies a gross motion of the bubble or drop and not a perturbation of the leading interface. Such a disturbance is considered not to cause a particle disintegration. Therefore, instead of the most unstable wave, we propose here to consider the wave which makes the left hand side of Eq. (47) maximum. Then at this condition the maximum stable particle size can be determined. Hence, the maximum diameter is given by the following equation

$$(k_m c_i)\left[\frac{\rho_c + \rho_d \coth(k_m h_d)}{\rho_c u_c}\right](d_p)_{max} \ln\left[\frac{\tan(\theta_\omega/2)}{\tan(\theta_o/2)}\right] = \ln(\eta_b/\eta') \tag{49}$$

where k_m is determined by

$$\frac{\partial}{\partial k}\left\{(kc_i)\left[\frac{\rho_c + \rho_d \coth(kh_d)}{\rho_c u_c}\right]\ln\left[\frac{\tan(\theta_\omega/2)}{\tan(\theta_o/2)}\right]\right\} = 0 \tag{50}$$

where kc_i and h_d are given by Eqs. (41) and (42), respectively, with $\theta = \theta_o$.

Variables such as θ_ω, θ_o, u_c and $\ell n\,(\eta_b/\eta')$ are evaluated below and several important conclusions are obtained.

1. Wake Angle

Large fluid particles which are prone to splitting have been studied in some detail previously, and several transition criteria for fluid particle shape regimes have been proposed [30]. When these studies are compared with available experimental breakup data it is seen that drops falling in gases and drops in a liquid system never reach the spherical-cap particle regime. However, very large bubbles in the order of 10 cm and most bubbles at the breakup point attain the spherical-cap shape. Therefore, in our analysis for the maximum diameter, each of the experimental data is checked with the shape regime criteria suggested by Clift et al. If the particle falls into spherical-cap shape regime, the wake angle of $\theta_\omega = 50°$ is used in Eq. (47). On the other hand, if the particle falls into spherical or ellipsoidal shape particle regime then $\theta_\omega = 90°$ is used in Eq. (47).

2. Particle Diameter and Volume Equivalent Diameter

In most drop or bubble experiments, data are tabulated in terms of the volume equivalent diameter, d_e, rather than based on the mean curvature diameter, d_p. Therefore, it is desirable to express the criterion in terms of d_e. Referring to Fig. 2, it can be shown that

$$d_p = \left[\frac{4}{(1 - \cos\theta_\omega)^2\,(2 + \cos\theta_\omega)}\right]^{1/3} d_e \tag{51}$$

Hence, d_p appearing in the criterion set above can be replaced by d_e through

$$d_p = c_e\, d_e \tag{52}$$

where

$$c_e = \left[\frac{4}{(1 - \cos\theta_\omega)^2\,(2 + \cos\theta_\omega)}\right]^{1/3}$$

for spherical-cap shaped particles.

3. Angular Position of Disturbance Generation

From Eq. (45) it is evident that disturbances which originated at the axis of symmetry, i.e., at $\theta_o = 0$, would never reach the end of the cap bubble or the equator of spherical particles. They are purely standing waves in nature. Observations of splitting bubble experiments performed by Clift et al. [27] indicated that disturbances usually develop in a regular pattern to either side of the leading nose. There are two fundamental patterns which may be possible.

Case A. The bubble nose is a node when the initial disturbance originates, then

$$\theta_o = \frac{\lambda}{2 d_p} = \frac{\pi}{k d_p} \tag{53}$$

Case B. A node is located $\lambda/4$ from the bubble nose so that the nose is an antinode in the initial disturbance form, then

$$\theta_o = \frac{\lambda}{d_p} = \frac{2\pi}{k d_p} \tag{54}$$

In Case A, the disturbance originated closer to the bubble nose than in B, thus yielding longer available times and, therefore, Case A was preferred by Clift et al. However, Case B yields an axisymmetric propagation which is considered to be more realistic, thus Case B is chosen here. Hence,

$$\theta_o = \frac{2\pi}{k c_e d_e} \tag{55}$$

will be used throughout analysis.

4. Terminal Velocity

There is a substantial body of data in the literature on the terminal velocity of a single bubble or drop. From these data many correlations for

calculating the velocity, u_c, are developed [31,38-42]. Similar studies have also been carried out for multiparticle systems [43]. The terminal velocity correlations were reviewed in detail by Grace et al. [42]. In our analysis we used the correlations recommended by them. These are given below:

1. For drops falling through gas

$$u_c = 2.0 \left(\frac{g|\Delta\rho|\sigma}{\rho_c^2} \right)^{1/4} \tag{55}$$

2. For large bubbles rising through liquid

$$u_c = 1.7 \left(\frac{g|\Delta\rho|d_e}{\rho_c} \right)^{1/2} \tag{56}$$

3. For drops rising or falling through liquid

$$u_c = 0.5 \left(\frac{\mu_c}{\rho_c d_e} \right) \left[(F^2 + 2\,Ar)^{1/2} - F \right] \quad \text{for } M > 0.01 \tag{57}$$

where M and Ar are Morton number and Archimedes number, respectively. They are defined as

$$M = \frac{g\,\mu_c^4\,|\Delta\rho|}{\rho_c^2\,\sigma^3} \tag{58}$$

$$Ar = \frac{g\,|\Delta\rho|\,\rho_c\,d_e^3}{\mu_c^2} \tag{59}$$

and parameter F is given by

$$F = \frac{3\,[2 + (\mu_d/\mu_c)]}{1 + (\mu_d/\mu_c)} \tag{60}$$

On the other hand,

$$u_c = \left(\frac{\mu_c}{\rho_c d_e}\right)(Y - 0.859)\, M^{-0.149} \quad \text{for } M < 0.001 \text{ and } E_o < 40 \tag{61}$$

where Y is a property group defined by

$$Y = 0.94\, H^{0.757} \qquad \text{for } 2 \leq H \leq 59.3 \tag{62}$$

or

$$Y = 3.42\, H^{0.441} \qquad \text{for } H > 59.3 \tag{63}$$

Here H is given by

$$H = \frac{4}{3} Eo\, M^{-0.149}\, (\mu_c/\mu_\omega) \tag{64}$$

with μ_ω taken as 0.9×10^{-3} Ns/m^2 and Eo is Eötvös number defined by

$$Eo = \frac{g\, \Delta\rho\, d_e^2}{\sigma} \tag{65}$$

C. Breakup Correlation

It is evident from Eqs. (49) and (50) that in order to arrive at a predictive criterion, one needs to know the relative magnitude of the initial disturbance, (η_b/η'). In order to explicitely determine this quantity it is necessary to resort to experiments. A reasonable approach is to correlate this term in terms of basic variables affecting η_b and η'. It is to be noted that η_b, the amplitude of progressing waves at the breakup, should be in the

order of a particle diameter. On the other hand, the initial disturbance amplitude, η', must be a strong function of the rise or fall velocity. Furthermore, considering that the density ratio varies few orders of magnitude between liquid-gas and gas-liquid systems, a reasonble correlation may be sought in the form of

$$\ell n\ (\eta_b/\eta') = f\ (d_e,\ u_c,\ \rho_c/\rho_d) \tag{66}$$

In view of Eqs. (52), (54) and (66), Eq. (49) can be cast into a non-dimensional form as follows:

$$(k_m^* c_i^*)\left(\frac{\rho^* + \coth(k_m^* h_d^*)}{\rho^*\ u_c^*}\right) c_e (d_e)^*_{max}\ \ell n\left[\frac{\tan(\theta_\omega/2)}{\tan\left(\pi/k_m^* c_e d_{e_{max}}^*\right)}\right] = f[(d_e^*)_{max},\ u_c^*,\ \rho^*] \tag{67}$$

where starred quantities denote the dimensionless variables. They are defined as follows:

$$(d_e)^*_{max} \equiv \frac{(d_e)_{max}}{(\sigma/g\ |\Delta\rho|)^{1/2}}$$

$$k_m^* \equiv k\left(\frac{\sigma}{g|\Delta\rho|}\right)^{1/2}$$

$$h_d^* \equiv \frac{h_d}{(\sigma/g\ |\Delta\rho|)^{1/2}} \tag{68}$$

$$u_c^* \equiv \frac{u_c}{(g|\Delta\rho|(d_e)_{max}/\rho_c)^{1/2}}$$

$$c_i^* \equiv \frac{c_i}{\left(g|\Delta\rho|(d_e)_{max}/\rho_c\right)^{1/2}}$$

$$\rho^* \equiv \frac{\rho_c}{\rho_d}$$

Now the dimensionless growth factor is obtained from Eq. (41) as

$$k_m^* c_i^* = \left\{ \frac{\rho^* \coth(k^* h_d^*)\left[\frac{3}{2} u_c^* \sin\left(\frac{2\pi}{k_m^* c_e^* (d_e^*)_{max}}\right)\right]^2 k^{*2}}{\left[\rho^* + \coth(k_m^* h_d^*)\right]^2} - \left[\frac{\rho^* k_m^*}{(d_e^*)_{max}}\right] \frac{(k^{*2} - 1)}{\rho^* + \coth(k_m^* h_d^*)} \right\}^{1/2} \tag{69}$$

In these equations, the dimensionless wave number, k_m, is determined by Eq. (50), which in dimensionless form becomes

$$\frac{\partial}{\partial k^*}\left\{(k^* c_i^*)\left[\frac{\rho^* + \coth(k^* h_d^*)}{\rho^* u_c^*}\right] \ln\left[\frac{\tan(\theta_\omega/2)}{\tan(2\pi/k^* c_e^* (d_e^*)_{max})}\right]\right\} = 0 \tag{70}$$

Using substantial amounts of data tabulated in Table I the nondimensional form of function f is correlated. For this purpose the linear regression analysis is used, and the best fit is expressed by the following function,

$$f[(d_e^*)_{max},\ u_c^*,\ \rho^*] = 0.0545\ \frac{(d_e)_{max}^{*1.340}}{\left[u_c^*\ \frac{\rho^*}{1+\rho^*}\right]^{0.6975}} \qquad (71)$$

Together with Eq. (71), Eq. (65) determines the maximum particle diameter at breakup. The correlation found here is general in the sense it can be applicable for liquid-gas, liquid-liquid, and gas-liquid systems for relatively low viscous fluids because the viscosity effects have been neglected to arrive at the correlation.

V. COMPARISON BETWEEN THEORY AND EXPERIMENTS

Predicted values of $(d_e)_{max}$ are compared against experimental values in Table I and Fig. 3. It is evident from the table that the experimental data cover a broad range of liquid-liquid, liquid-gas and gas-liquid systems. The results include the data by Hu and Kintner [31], Krishna et al. [33] and Grace et al. [29] for liquid-liquid systems, by Merrington and Richardson [3], Finlay [32] and Ryan [35] for liquid drops falling through gas, and finally by Grace et al. [3] and Sundell [34] for rising bubbles through stagnant liquid. In addition to the experimental and predicted values of $(d_e)_{max}$, the deviation between predicted and experimental values of $(d_e)_{max}$ and the mean deviation for each group are also listed in Table I.

The average deviation between predicted and experimental value of $(d_e)_{max}$ varies from about 3.65% for Ryan data to 31.90% for Hu and Kintner data with an overall mean deviation of 18.06%. Four of the systems studied by Hu and Kintner are in common with systems investigated by Krishna et al., while two of the Finlay systems are essentially identical with Merrington and Richardson systems. However, the mean deviation changes drastically between Hu and Kintner and Krishna et al. data and between Merrington and Richardson and Finlay data. Although there are some differences in reported values of fluid properties, a significant part of the discrepancy between predictions and theory arises from experimental scatter or bias. It is to be noted that the Hu and Kintner data having the largest mean deviation show diameters to be consistently lower than the theoretical ones.

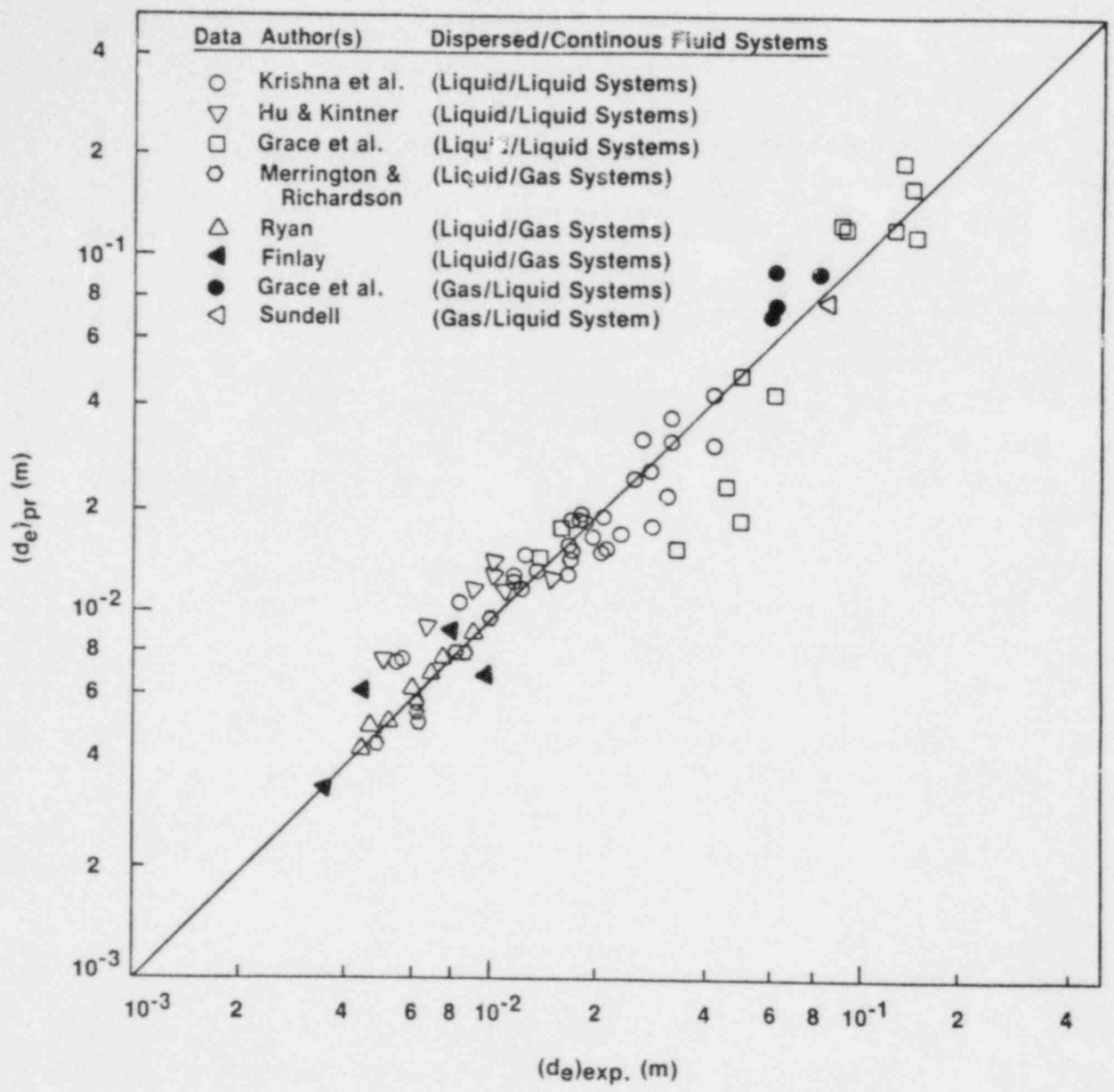

Fig. 3. Comparison Between Experimental Maximum Diameters with Predictions

Relatively large differences between the predicted diameters and the Grace et al. data for liquid-liquid systems may be due to viscosity effects of the continuous fluid. Grace et al. experiments cover a dynamic viscosity range of 12.4 to 3080 Ns/m. In our analysis as mentioned above viscous effects have been neglected. Therefore, the present correlation may not be very good for highly viscous fluids.

Taking the experimental scatter and the very viscous fluids used for some experiments into consideration, and recalling the approximate nature of the theory developed here, the agreement between the theoretical predictions and the experimental results is satisfactory. The overall mean deviation between the predicted and experimental values of $(d_e)_{max}$ is ± 18.06%. Agreements with experimental results indicates that the principle physical mechanisms involved are properly accounted for.

VI. SUMMARY AND CONCLUSIONS

Two-dimensional Kelvin-Helmholtz instability is applied to the stability of two superposed fluids flowing with different velocities. The stability criterion implies that stability of disturbances is a function of the wave number, amplitude, relative velocity and the original amplitude of disturbances at the interface. Based on this stability theory, a simple model is developed to describe the breakup of drops and bubbles falling or rising freely in a fluid media. Breakup is predicted to occur if the growth of disturbances on the leading front is rapid enough compared to the rate at which the disturbance is propagated along the interface. Using the available experimental data for liquid-gas, liquid-liquid and gas-liquid systems a simple semi-empirical correlation is developed to predict the maximum stable particle size in a stagnant fluid.

Predicted values of the maximum particle size are compared with experimental data. An average deviation between the predicted and experimental values is 18%. Considering the various simplifications made in the analysis the agreement appears satisfactory. The theoretical model developed in this study is clearly approximate in nature. However, the agreement with experimental results over very wide ranges of parameters indicates that the principle physical mechanisms involved are properly accounted for by the present model. Therefore, the breakup of bubbles and drops can be explained by the present unified theory.

ACKNOWLEDGMENTS

The authors would like to express their appreciation to Dr. N. Zuber and Mr. M. Young of NRC for valuable discussions on the subject.

This work was performed under the auspices of the U. S. Nuclear Regulatory Commission.

REFERENCES

1. Lenard, P., "Ueber Regen," Meteor. Zeit., Vol. 21, pp. 248-262 (1904).

2. Hochschwender, Z., Ph.D. Thesis, Univ. of Heidelberg, Germany (1919).

3. Merrington, A. C. and Richardson, E. G., "The Break-Up of Liquid Jets," Proc. Phys. Soc. (London), Vol. 59, pp. 1-13 (1947).

4. Hinze, J. O., "Critical Speeds and Sizes of Liquid Globules," Appl. Sci. Res., A.1, pp. 273-281 (1948).

5. Hanson, A. R., Domich, E. G., and Adams, H. S., "Shock Tube Investigation of the Breakup of Drops by Air Blasts," Phys. Fluids, Vol. 6, pp. 1070-1080 (1963).

6. Lane, W. R., "Shatter of Drops in Streams of Air," Ind. Eng. Chem., Vol. 43, pp. 1312-1317 (1951).

7. Hinze, J. O., "Fundamentals of the Hydrodynamic Mechanism of Splitting in Dispersion Processes," AIChE J. Vol. 1, pp. 289-295 (1955).

8. Haas, F. C., "Stability of Droplets Suddenly Exposed to a High Velocity Gas Stream," AIChE J., Vol. 10, pp. 920-924 (1964).

9. Harper, E. Y., Grube, G. W., and Chang, I., "On the Breakup of Accelerating Liquid Drops," J. Fluid Mech., Vol. 52, pp. 565-591 (1972).

10. Brodkey, R. S., The Phenomena of Fluid Motions, Addison-Wesley Pub. Co. (1967).

11. Taylor, G. E., "The Function of Emulsion in Definable Field Flow," Proc. Roy. Soc. (London), Series A, Vol. 146, pp. 501-523 (1934).

12. Tomotika, S., "Breaking Up of a Drop of Viscous Liquid Immersed in Another Viscous Fluid Which is Extending at a Uniform Rate," Proc. Roy. Soc. (London), Series A, Vol. 153, pp. 302-320 (1936).

13. Rumscheidt, F. D. and Mason, S. G., "Particle Motion in Sheared Suspensions, XII. Deformation and Burst of Fluid Drops in Shear and Hyperbolic Flows," J. Colloid Sci., Vol. 16, pp. 238-261 (1967).

14. Karam, H. J. and Bellinger, J. C., "Deformation and Breakup of Liquid Droplets in a Simple Shear Field," Ind. Eng. Chem. Fundam., Vol. 7, pp. 576-581 (1968).

15. Buckmaster, J. D., "The Bursting of Pointed Drops in Slow Viscous Flow," J. Appl. Mech., Vol. 40, pp. 18-24 (1973).

16. Kolmogorov, A. N., "On the Disintegration of Drops in a Turbulent Flow," Doklady Akad. Nauk, SSSR, Vol. 66, p. 825 (1949).

17. Clay, P. H., Proc. Roy. Acad. Science (Amsterdam), Vol. 43, p. 852 (1940).

18. Sleicher, C. A., "Maximum Drop Size in Turbulent Flow," AIChE J., Vol. 8, pp. 471-477 (1962).

19. Sevik, M. and Park, S. H., "The Spliting of Drops and Bubbles by Turbulent Fluid Flow," J. Fluids Eng., Vol. 95, pp. 53-60 (1973).

20. Komaboyashi, M., Gonda, T., and Isono, K., "Lifetime of Water Drops Before Breaking and Size Distribution of Fragment Drops," J. Meteor. Soc. Japan, Ser. 2, Vol. 42, pp. 330-340 (1964).

21. Pruppacher, H. R. and Pitter, R. L., "A Semi-Empirical Determination of the Shape of Cloud and Rain Drops," J. Atmos. Sci., Vol. 28, pp. 86-94 (1971).

22. Blanchard, D. C., "The Behavior of Water Drops at Terminal Velocity," Trans. Amer. Geophys. Union, Vol. 31, pp. 836-842 (1950).

23. Blanchard, D. C., "Comments on the Breakup of Raindrops," J. Atmos. Sci., Vol. 19, pp. 119-120 (1962).

24. Cotton, W. R. and Gokhale, N. R., "Collision, Coalescence and Breakup of Large Water Drops in a Vertical Wind Tunnel," J. Geophys. Res., Vol. 72, pp. 4041-4049 (1967).

25. Klett, J. D., "On the Breakup of Water Drops in Air," J. Atmos. Sci., Vol. 28, pp. 646-647 (1971).

26. Clift, R. and Grace, J. R., "The Mechanisms of bubble Breakup in Fluidized Beds," Chem. Eng. Sci., Vol. 27, pp. 2309-2310 (1973).

27. Clift, R., Grace, J. R., and Weber, M. E., "Stability of Bubbles in Fluidized Beds," Ind. Eng. Chem. Fundam., Vol. 13, pp. 45-51 (1974).

28. Henricksen, H. K. and Øtergaard, K., "On the Mechanism of Breakup of Large Bubbles in Liquids on Three-Phase Fluidized Beds," Chem. Eng. Sci., Vol. 29, pp. 626-629 (1974).

29. Grace, J. R., Wairegi, T., and Brophy, J., "Break-up of Drops and Bubbles in Stagnant Media," Can. J. Chem. Eng., Vol. 56, pp. 3-8 (1978).

30. Clift, R., Grace, J. R., and Weber, M. E., Bubbles, Drops and Particles, Academic Press, New York (1978).

31. Hu, S. and Kintner, R. C., "The Fall of Single Liquid Drops Through Water," AIChE J., Vol. 1, pp. 43-49 (1955).

32. Finlay, B. A., Ph.D. Thesis, Univ. Birmingham (1957).

33. Krishna, P. M., Venkateswarlu, D., and Narasimhamurty, G. S. R., "Fall of Liquid Drops in Water, Terminal Velocities," J. Chem. Eng. Data, Vol. 4, pp. 336-343 (1959).

34. Sundell, R. E., Ph.D. Thesis, Yale Univ. (1971).

35. Ryan, R. T., "The Possible Modification of Convective Systems by the Use of Surfactants," J. Appl. Meteor., Vol. 15, pp. 3-8 (1978).

36. Yih, C. H., Stratified Flows, Academic Press, Second Edition (1980).

37. Lamb, H., Hydrodynamics, Dover Publications, Sixth Edition (1945).

38. Klee, A. J. and Treyball, R. E., "Rate of Rise of Fall of Liquid Drops," AIChE J., Vol. 2, pp. 444-447 (1956).

39 Mendelson, H. D., "Prediction of Bubble Terminal Velocities from Wave Theory," AIChE J., Vol. 13, pp. 250-252 (1967).

40 Marruici, G., Apuzzo, G., and Astarita, G., "Motion of Liquid Drops in Non-Newtonian Systems," AIChE J., Vol. 16, pp. 538-541 (1970).

41. Wallis, G. B., "The Terminal Speed of Single Drops or Bubbles in an Infinite Medium," Int. J. Multiphase Flow, Vol. 1, pp. 491-511 (1974).

42. Grace, J. R., Wairegi, T., and Nguyen, T. H., "Shapes and Velocities of Single Drops and Bubbles Moving Freely Through Immiscible Fluids," Trans. Inst. Chem. Eng., Vol. 54, pp. 167-173 (1976).

43. Ishii, M. and Zuber, N., "Drag Coefficient and Relative Velocity in Bubbly, Droplet or Particulate Flows," AIChE J., Vol. 25, pp. 843-855 (1979).

Table I. Comparison Between Experimental Maximum Diameters with Predictions

System	Dispersed Fluid/Continuous Fluid	Properties					$(d_e)_{max} \times 10^3$ (m)		Deviation %	Mean Deviation %
		ρ_d (kg/m^3)	ρ_c (kg/m^3)	$\mu_d \times 10^3$ (Ns/m^2)	$\mu_c \times 10^3$ (Ns/m^2)	$\sigma \times 10^3$ (N/m)	Experimental	Predicted		
Liquid-Gas Systems	Merrington & Richardson [3]									
	water/air	1000	1.25	1.206	0.018	73.0	10.20	10.05	- 1.47	
	carbon tetrachloride/air	1600	1.25	0.960	0.018	25.0	4.80	4.60	- 4.17	
	methyl salicylate/air	1330	1.25	3.990	0.018	35.0	6.20	5.80	- 6.45	
	glyceine + 2% water/air	1210	1.25	121.0	0.018	63.7	8.80	8.41	- 4.43	8.07
	methyl salicylate (thick)/air	1330	1.25	0.532	0.018	30.0	6.40	5.40	+15.62	
	tetrabromoethane/air	1340	1.25	938.0	0.018	25.0	6.40	4.90	-23.43	
	dirty water/air	981	1.25	1.2	0.018	48.0	8.40	8.48	+ 0.95	
	Ryan [35]									
	water/air	998	1.18	1.044	0.018	72.0	9.10	9.40	+ 3.30	
	water + surfactant/air	998	1.18	1.004	0.018	50.0	7.50	7.90	+ 5.33	
	water + surfactant/air	998	1.18	1.004	0.018	40.0	6.90	7.20	+ 4.35	
	water + surfactant/air	998	1.18	1.004	0.018	33.0	6.10	6.50	+ 6.56	3.65
	water + surfactant/air	998	1.18	1.004	0.018	25.0	5.20	5.20	0.00	
	water + surfactant/air	998	1.18	1.004	0.018	20.0	4.70	4.93	+ 4.89	
	water + surfactant/air	998	1.18	1.004	0.018	17.0	4.40	4.45	+ 1.14	
	Finley [32]									
	tetrabromoethane/air	2968	1.18	11.52	0.018	50.0	3.50	3.41	- 2.57	
	isobutanol/air	998	1.18	1.044	0.018	73.5	8.00	9.38	+17.25	
	water/air	1200	1.18	124.2	0.018	63.0	10.00	7.10	-29.00	22.21
	glycerol solution/air	803	1.18	4.14	0.018	23.0	4.50	6.30	+40.00	

Table I. (Cont'd)

System	Dispersed Fluid/Continuous Fluid	Properties ρ_d (kg/m^3)	ρ_c (kg/m^3)	$\mu_d \times 10^3$ (Ns/m^2)	$\mu_c \times 10^3$ (Ns/m^2)	$\sigma \times 10^3$ (N/m)	$(d_e)_{max} \times 10^3$ (m) Experimental	Predicted	Deviation %	Mean Deviation %
Liquid-Liquid Systems	Krishna et al. [33]									
	n-amyl phthalate/water	1016	998.1	18.490	0.828	20.20	42.40	43.48	+ 2.54	
	aniline/water	1016	998.1	2.835	0.820	6.545	27.00	26.30	- 2.59	
	bromoform/water	2850	998.9	2.127	0.9156	40.60	5.60	7.78	+38.92	
	n-butyl phthalate/water	1044	998.1	15.38	0.9499	23.61	42.40	31.60	-25.47	
	carbon disulfide/water	1260	999.1	0.6531	0.9499	45.67	16.70	16.50	- 1.20	
	carbon tetrachloride/water	1584	998.9	1.048	0.9156	44.66	11.80	13.26	+12.37	
	clorobenzene/water	1096	998.1	0.7861	0.828	36.02	31.60	22.50	-28.80	
	1-chlorobenzene/water	1200	995.3	2.289	0.766	41.90	19.70	17.01	-13.65	
	m-cresol/water	1028	998.1	7.732	0.828	4.134	17.90	13.62	-23.91	
	epichlorohydrin/water	1169	997.5	0.9116	0.8085	10.98	12.40	12.40	0.0	
	ethyl chloroacetate/water	1134	996.1	0.9642	0.7848	15.46	13.70	13.70	0.0	
	ethyl cinnamate/water	1042	998.1	4.811	0.828	21.68	27.10	32.30	-19.19	
	ethyl phthalate/water	1128	999.5	10.86	0.9759	14.40	16.80	15.25	- 9.23	
	1,2-dibromoethylene/water	2170	998.9	1.752	0.9156	36.58	8.30	11.30	+36.14	
	eugenol/water	1058	998.1	5.43	0.828	12.34	17.30	19.40	+12.14	15.29
	isoeugenol/water	1083	999.1	27.06	0.9499	9.38	16.80	16.17	- 3.75	
	methyl phthalate/water	1180	996.1	9.383	0.7848	12.26	11.80	13.00	+10.17	
	nitrobenzene/water	1195	997.5	1.512	0.8085	24.81	17.90	19.41	+ 8.44	
	m-nitrotoluene/water	1156	999.3	2.044	0.9594	28.38	21.20	15.96	-24.72	
	o-nitrotolune/water	1153	996.1	1.666	0.7848	26.03	21.20	19.81	- 6.56	
	diphenyl ether/water	1067	996.1	2.633	0.7848	40.80	32.50	37.43	+15.17	
	1,2-dichloropropene/water	1146	995.8	0.7966	0.785	31.11	23.50	18.05	-23.19	
	1,1,2,2-tetrabromoethane/water	2939	996.0	5.495	0.7805	33.35	5.50	7.72	+40.36	
	1,1,2,2-tetrachloroethane/water	1581	998.1	1.452	0.828	30.09	11.00	13.78	+25.27	
	tetrachloroethylene/water	1609	996.1	0.9497	0.7848	43.38	12.70	15.23	+19.92	
	n-amyl phthalate/water	1016	998.1	16.38	0.828	7.071	32.50	32.50	0.0	
	chlorobenzene/water	1088	998.0	0.7877	0.828	25.54	26.00	25.41	- 2.27	
	chlorobenzene/water	1072	998.0	0.7637	0.828	19.56	28.00	18.78	-32.92	
	chlorobenzene/water	1072	998.0	0.7716	0.828	14.07	21.00	16.31	-23.33	
	chlorobenzene/water	1073	998.0	0.7843	0.828	9.143	18.70	19.35	+ 3.48	
	nitrobenzene/water	1157	998.1	1.838	0.828	15.84	18.00	19.56	+ 8.67	

Table I. (Cont'd)

System	Dispersed Fluid/Continuous Fluid	Properties					$(d_e)_{max} \times 10^3$ (m)		Deviation %	Mean Deviation %
		ρ_d (kg/m^3)	ρ_c (kg/m^3)	$\mu_d \times 10^3$ (Ns/m^2)	$\mu_c \times 10^3$ (Ns/m^2)	$\sigma \times 10^3$ (N/m)	Experimental	Predicted		
Liquid-Liquid Systems	Hu & Kintner [31]									
	tetrabromoethane/water	2947.4	997.3	9.2888	0.8968	35.90	5.11	7.81	+52.84	
	dibromoethane/water	2154.1	996.6	1.5852	0.8968	31.90	6.74	9.59	+42.28	
	ethyl bromide/water	1447.8	997.7	0.4908	0.8814	30.00	9.14	12.27	+34.25	
	nitrobenzene/water	1194.7	997.2	1.7379	0.8835	24.10	15.37	13.28	-13.60	31.90
	bramobenzene/water	1488.1	997.1	1.0719	0.8958	37.90	11.32	12.30	+ 8.66	
	tetrachloroethylene/water	1614.3	997.0	0.8903	0.8946	44.3	10.40	14.65	+40.87	
	carbon tetrachloride/water	1577.0	995.7	0.8702	0.7797	40.6	10.40	13.60	+30.77	
	Grace et al. [29]									
	carbon tetrachloride/sugar solution	1586	1382	1.05	3080	34.4	135.00	127.10	- 5.92	
	carbon tetrachloride/sugar solution	1586	1388	1.05	1200	34.4	156.00	121.90	-21.86	
	chloroform/sugar solution	1483	1382	0.56	3080	32.7	142.00	191.10	+34.51	
	chloroform/sugar solution	1483	1387	0.51	1520	32.8	151.00	166.30	+10.13	
	chloroform/sugar solution	1483	1366	0.56	300	31.9	63.00	43.21	-31.41	
	chloroform/sugar solution	1483	1310	0.56	54	31.4	34.00	16.20	-52.35	26.73
	1,2-dichloroethane/ethylene glycol	1247	1112	1.04	14.8	6.94	14.20	14.90	+ 4.93	
	glycerol solution/paraffin oil	1062	883	2.0	185	51.0	51.00	49.22	- 3.49	
	silicone oil/ethylene glycol	958	1112	46.5	12.4	24.0	16.20	18.24	+12.59	
	silicone oil/paraffin oil	960	883	46.5	200	7.0	51.00	19.20	-62.35	
	silicone oil/sugar solution	958	1366	46.5	310	27.1	46.00	24.33	-47.11	
	silicone oil/sugar solution	920	1390	5.5	2890	53.5	99.00	122.80	+24.04	
	silicone oil/sugar solution	920	1390	6.1	2700	53.5	95.00	130.00	+36.84	

Distribution for NUREG/CR-4028 (ANL-84-67)

Internal:

C. E. Till
R. Avery
J. F. Marchaterre
A. J. Goldman
P. A. Lottes
L. W. Deitrich
D. Rose
D. H. Cho
H. Komoriya
B. W. Spencer
W. A. Ragland
G. DeJarlais
D. P. Weber
W. T. Sha
Y. W. Shin
J. Sienicki
W. L. Chen
T. C. Chawla
T. Y. Wei
A. M. Tentner
M. Ishii (20)
ANL Patent Dept.
ANL Contract File
ANL Libraries (2)
TIS Files (6)

External:

NRC Washington, for distribution per R2 and R4 (335)
DOE-TIC (2)
Manager, Chicago Operations Office, DOE
Reactor Analysis and Safety Division Review Committee:

W. B. Behnke, Jr., Commonwealth Edison Co., P. O. Box 767, Chicago, Ill. 60690
W. P. Chernock, Combustion Engineering, Inc., 1000 Prospect Hill Road, Windsor, Conn. 06095
W. M. Jacobi, Westinghouse Electric Corp., P. O. Box 355, Pittsburgh, Pa. 15230
S. Levine, NUS Corp., 910 Clopper, Gaithersburg, Md. 20878
E. A. Mason, Standard Oil Co., P. O. Box 400, Naperville, Ill. 60566
W. F. Miller, Jr., Los Alamos National Lab., Los Alamos, N. M. 87545
M. J. Ohanian, University of Florida, Gainesville, Fla. 32611
J. J. Taylor, Electric Power Research Inst., P. O. Box 10412, Palo Alto, Calif. 94303

NRC FORM 335 (2 84) NRCM 1102, 3201, 3202

U.S. NUCLEAR REGULATORY COMMISSION

BIBLIOGRAPHIC DATA SHEET

See INSTRUCTIONS ON THE REVERSE

1. REPORT NUMBER (Assigned by TIDC add Vol. No., if any)

NUREG/CR-4028
ANL-84-67

2. TITLE AND SUBTITLE

Unified Theory for Predicting Maximum Fluid Particle Size for Drops and Bubbles

3. LEAVE BLANK

4. DATE REPORT COMPLETED

MONTH	YEAR
June	1984

5. AUTHOR(S)

G. Kocamustafaogullari, I. Y. Chen, and M. Ishii

6. DATE REPORT ISSUED

MONTH	YEAR
October	1984

7. PERFORMING ORGANIZATION NAME AND MAILING ADDRESS (Include Zip Code)

Argonne National Laboratory
9700 South Cass Avenue
Argonne, Illinois 60439

8. PROJECT/TASK/WORK UNIT NUMBER

8M406

9. FIN OR GRANT NUMBER

A2026

10. SPONSORING ORGANIZATION NAME AND MAILING ADDRESS (Include Zip Code)

Division of Accident Evaluation
Office of Nuclear Regulatory Research
U.S. Nuclear Regulatory Commission
Washington, D. C. 20555

11a. TYPE OF REPORT

Technical

b. PERIOD COVERED (Inclusive dates)

FY 1984

12. SUPPLEMENTARY NOTES

13. ABSTRACT (200 words or less)

A simple model is developed based on a two-dimensional linearized Kelvin-Helmholtz stability theory to describe the breakup of drops and bubbles in fluid media. Breakup is predicted to occur if the growth of disturbances at the interface is faster than the rate at which disturbances propagate around the interface to the side of particle. Agreement between the model and experimental data indicates that the principle physical mechanisms involved are properly accounted for by the model. The same theory is applicable to drops in liquid, drops in gas, and bubbles in liquid. The present analysis gives the first unified theory for fluid particle breakups which has not been available previously.

14. DOCUMENT ANALYSIS - a. KEYWORDS/DESCRIPTORS

Two-phase Flow
Fluid Particle Size
Bubbly Flow

b. IDENTIFIERS/OPEN-ENDED TERMS

15. AVAILABILITY STATEMENT

Unlimited

16. SECURITY CLASSIFICATION

(This page) Unclassified

(This report) Unclassified

17. NUMBER OF PAGES

18. PRICE